



**HAL**  
open science

# Forced response prediction of a mistuned bladed disk in the presence of aeroelastic coupling and model uncertainties

Jean de Cazenove, Scott Cogan, Moustapha Mbaye, Marc Berthillier

## ► To cite this version:

Jean de Cazenove, Scott Cogan, Moustapha Mbaye, Marc Berthillier. Forced response prediction of a mistuned bladed disk in the presence of aeroelastic coupling and model uncertainties. International Conference on Vibrations in Rotating Machinery, Sep 2012, London, United Kingdom. pp.281-291, 10.1533/9780857094537.4.281 . hal-02300608

**HAL Id: hal-02300608**

**<https://hal.science/hal-02300608>**

Submitted on 18 Mar 2024

**HAL** is a multi-disciplinary open access archive for the deposit and dissemination of scientific research documents, whether they are published or not. The documents may come from teaching and research institutions in France or abroad, or from public or private research centers.

L'archive ouverte pluridisciplinaire **HAL**, est destinée au dépôt et à la diffusion de documents scientifiques de niveau recherche, publiés ou non, émanant des établissements d'enseignement et de recherche français ou étrangers, des laboratoires publics ou privés.

# Forced response prediction of a mistuned bladed disk in the presence of aeroelastic coupling and model uncertainties

J de Cazenove<sup>1,2</sup>, S Cogan<sup>1</sup>, M Mbaye<sup>2</sup>, M Berthillier<sup>1</sup>

<sup>1</sup> FEMTO-ST Institute, Applied Mechanics - UMR CNRS 6174, France

<sup>2</sup> Turbomeca, France

## ABSTRACT

The present study focuses on a sensitivity analysis of uncertain parameters for a mistuned bladed disk. After providing a general overview of the main theoretical aspects, this paper describes the way of computing the forced response with aeromechanical coupling. The bladed disk considered here is a representative naturally mistuned bladed disk whose geometry has been obtained by scan. A global sensitivity analysis is then performed using the Morris algorithm in order to rank a set of conservative and dissipative uncertain parameters in terms of their influence on the forced response level. Since a large number of response computations are needed for the sensitivity analysis, a reduced-order model that encompasses geometric mistuning is used.

## NOMENCLATURE

|                                |  |
|--------------------------------|--|
| $[K]$                          | <i>Structural stiffness matrix</i>                               |
| $[M]$                          | <i>Mass matrix</i>   |
| $[C]$                          | <i>Structural damping matrix</i>                                 |
| $i$                            | <i>Imaginary unit</i>  |
| $\omega$                       | <i>Angular frequency</i>   |
| $u(\omega)$                    | <i>Displacement field in the frequency domain</i>                |
| $f_{exc}(\omega)$              | <i>Aerodynamic excitation forces</i>                             |
| $f_{coupl}(\omega, u(\omega))$ | <i>Aeroelastic coupling forces</i>                               |
| $[K_L]$                        | <i>Linear structural stiffness matrix</i>                        |
| $\Omega$                       | <i>Rotation speed</i>  |
| $[M_c]$                        | <i>Centrifugal stiffness matrix</i>                              |
| $[K(\varepsilon)]$             | <i>Geometric stiffness matrix</i>                                |
| $F_c(\Omega^2)$                | <i>Centrifugal load under rotation speed <math>\Omega</math></i> |
| $[\Phi]$                       | <i>Modal reduction basis</i>                                     |
| $[\hat{\Phi}]$                 | <i>Modal reduction basis in the Fourier space</i>                |
| $a_{\beta,k}^*$                | <i>Aeroelastic complex coefficient</i>                           |
| $P^*(x, y, z)$                 | <i>Aerodynamic pressure field in the frequency domain</i>        |

|                                      |  |
|--------------------------------------|--|
| $\Phi_{\beta,k}(x, y, z)$            | <i>Modal displacement field</i>  |
| $\eta$                               | <i>Generalized coordinates</i>   |
| $Z$                                  | <i>Basis of eigenvectors of the conservative reduced system</i>                        |
| $\zeta$                              | <i>Modal damping ratio</i>   |
| $\lambda_i$                          | <i><math>i^{\text{th}}</math> eigenvalue of the conservative reduced system</i>        |
| $[A^*] = \text{diag}(a_{\beta,k}^*)$ | <i>Complex Generalized Aerodynamic Forces matrix</i>                                   |
| $[A^*]$                              | <i>Aeroelastic Influence Coefficients matrix</i>                                       |
| $E$                                  | <i>Complex Fourier matrix</i>  |
| $N$                                  | <i>Number of sectors</i>   |
| $[A_{per}^*]$                        | <i>Perturbed Aeroelastic Influence Coefficients matrix</i>                             |
| $[\hat{A}_{per}^*]$                  | <i>Perturbed Generalized Aerodynamic Forces matrix</i>                                 |
| $[A_{per}]$                          | <i>Perturbed aeroelastic stiffness matrix</i>  |
| $[B_{per}]$                          | <i>Perturbed aeroelastic damping matrix</i>  |
| $r$                                  | <i>Number of trajectories in the uncertain variables space</i>                         |
| $m$                                  | <i>Number of points for a given trajectory</i>   |
| $x$                                  | <i>Current point in the uncertain variables space</i>                                  |
| $d_i(x)$                             | <i>Sensitivity index associated to variable <math>i</math> at point <math>x</math></i> |
| $y(x)$                               | <i>Maximum amplification factor at point <math>x</math></i>                            |

### *Superscripts*

|     |   |
|-----|---|
| $r$ | <i>In the reduced modal coordinates</i> |
| $*$ | <i>Hermitian matrix</i>                 |
| $j$ | <i>Sector number</i>                    |

### *Subscripts*

|         |                       |
|---------|-----------------------|
| $\beta$ | <i>Mode family</i>    |
| $k$     | <i>Nodal diameter</i> |

## **1 INTRODUCTION**

It is well-known that turbomachine bladed disks undergo severe static and dynamic loads under operating conditions. Moreover, for most bladed disks, various resonant frequencies can be encountered in the operating frequency range. This results in an increase in the vibratory response, which may cause premature blade failure by high-cycle fatigue (HCF) [1,2]. In this context, numerical methods for predicting the forced response levels of bladed disk assemblies have been the focus of a large number of studies over the last few decades. Recent insights into the reduced-order modeling of bladed assemblies lead to compact and accurate models that can be used to predict forced response amplitudes under dynamic loads in operating conditions. However, the robustness of such prediction methods remains a key issue since several conservative and dissipative parameters are characterized by either random or epistemic uncertainties.

The dynamic behaviour of real bladed disks can be strongly modified by random mistuning. Mistuning results from manufacturing tolerances, non-homogeneity of

the material and wear, and it may cause significant increases in the forced response levels [3]. Reduced-order modeling of mistuned bladed disks requires specific methods and higher computational cost since the cyclic symmetry assumption is no longer valid. Surveys on the modeling of mistuned bladed disks are given in [4] and [2]. Recently, specific efforts have been devoted to the characterization of random, small geometric mistuning of real bladed disks. Sinha et al. [5] conducted a study over a population of Integrally Bladed Rotors (IBRs) for which the positions of various keypoints were measured for each blade by a Coordinate Measurement Machine (CMM). Schoenenborn et al. [6] studied the frequency mistuning pattern and dynamic behaviour of an IBR using a realistic FE model, based on an optical acquisition of the full disk geometry.

In addition to geometric and material mistuning, damping also plays a key role in the process of characterization of the forced response amplitudes. Damping in turbomachine bladed disks results from distinct physical phenomena, namely: material dissipation, frictional contact and aeromechanical coupling [7]. According to several studies, the material dissipation in most metals and alloys used for bladed disks manufacturing is small [8]. In the case of shroudless, integrally bladed disks, the aerodynamic damping is therefore the main source of dissipation since no frictional contact occurs.

The small geometric discrepancies between the blades also result into non-cyclic flows. Some studies investigated the losses of flow cyclicity by means of whole-annulus CFD calculations (see for example [9]), but due to the high computational cost, the computation of aeromechanical forces is generally performed under the hypothesis of chorochronicity. It is shown in some studies [10, 11] that under specific assumptions, interactions between blades through the flow can be considered to be limited to adjacent and next-to-adjacent blades, thus allowing the computation of non-cyclic aerodynamic generalized forces in the modal domain.

Ekici et al. [12] studied the effects of alternate blade spacing and stagger angle. In their study, the CFD calculations were performed on one sector composed of two adjacent blades, allowing the use of chorochronic boundary conditions and calculation of non-diagonal terms of the Generalized Aerodynamic Forces matrix. In this context, Miyakozawa and Kielb [13] recently carried out a study that focused on the Aeroelastic Influence Coefficients on which single, cyclic and random perturbations were applied. For the random case, a Monte-Carlo simulation was performed and the results showed that although frequency mistuning remains the dominant source of blade response amplification, aerodynamic asymmetric perturbations may also cause non-negligible increases in the maximum blade response levels.

The main objective of this paper is to investigate and classify the impact of several uncertain parameters (namely, the modulus of elasticity, the modal damping ratio and the Aeroelastic Influence Coefficients) on the maximum amplification factor for a mistuned bladed disk. All subsequent forced response calculations were performed using the reduced-order model of an industrial bladed disk whose geometry has been acquired by means of fringe projection. Thus, the model naturally takes into account small geometric mistuning which is observed on the manufactured bladed disk due to the manufacturing process. First, the main theoretical aspects for bladed disk forced response computation are presented. Afterwards, the expression of the projection basis used for the model reduction is given and the incidence of aerodynamic stiffness and damping on the forced response is demonstrated. The way of computing the deterministic forced response is then presented and subsequently, a parametric sensitivity study performed using the Morris method [14] is presented and its results are discussed.

## 2 THEORETICAL BACKGROUND

### 2.1 Dynamic equation of the mistuned system

In the frequency domain, taking into account the aeroelastic coupling, the aerodynamic excitation forces and neglecting the gyroscopic effects lead to the following expression of the dynamic equilibrium equation for the finite-element discretized system of the studied bladed disk:

$$([K] - \omega^2[M] + i\omega[C])u(\omega) = f_{exc}(\omega) + f_{coupl}(\omega, u(\omega)) \quad (1)$$

In equation (1),  $f_{exc}(\omega)$  and  $f_{coupl}(\omega, u(\omega))$  are namely the aerodynamic excitation forces vector due to flow interactions with the stator blades and the aeroelastic coupling forces vector, which represents the unsteady pressure induced by blade motion. It should be stressed that equation (1) is expressed in the rotating frame and that the effects of rotation are taken into account. Therefore the stiffness matrix  $[K]$  can be decomposed into 3 components as follows:

$$[K] = [K_L] - \Omega^2[M_c] + [K(\varepsilon)] \quad (2)$$

In equation (2)  $[K_L]$  corresponds to the classical, linear stiffness of the structure,  $[M_c]$  represents the additional stiffness matrix due to centrifugal effects, and  $[K(\varepsilon)]$  represents the prestress induced by the static component of the deformation field under centrifugal load [15, 16]. The expression of  $[K(\varepsilon)]$  is obtained through iterative resolution on the non-linear static problem which can be written as:

$$([K_L] - \Omega^2[M_c] + [K(\varepsilon)])u_0 = F_c(\Omega^2) \quad (3)$$

where  $F_c(\Omega^2)$  is the vector of centrifugal loads.

### 2.2 Reduction method

This section is devoted to the reduction method developed by Mbaye et al [17, 18] which has been applied to the studied mistuned blisk. This method is an extension of the *Subset of Nominal Modes* (SNM) method developed by Yang and Griffin [19]. Due to geometric mistuning, matrices  $[K]$  and  $[M]$  are no longer block-circulant and the projection of modified matrix blocks on nominal modes would result in non-negligible errors. The method used in this paper consists in building a reduction basis from the cyclic modes defined on each modified sector:

$$\Phi = \begin{pmatrix} \Phi_1^{\Gamma_1} & \dots & \Phi_{\alpha^*}^{\Gamma_1} \\ \vdots & \ddots & \vdots \\ \Phi_1^{\Gamma_N} & \dots & \Phi_{\alpha^*}^{\Gamma_N} \end{pmatrix} \quad (4)$$

$$\Phi_{\beta,k}^{\Gamma_j} = \hat{\Phi}_{\beta,k} \cos\left(\frac{2\pi j k}{N}\right) - \hat{\Phi}_{\beta,k} \sin\left(\frac{2\pi j k}{N}\right) \quad (5)$$

The components of the  $[\Phi]$  matrix in equation 4 are real modes, obtained from the Fourier modes  $[\hat{\Phi}_{\beta,k}^{\Gamma_j}]$  (see equation 5) where the indices  $j$ ,  $\beta$  and  $k$  correspond to the sector number, mode family (ex: 2F, 1T...) and nodal diameter, namely. The subscript indices  $(1, \dots, \alpha^*)$  in equation (4) correspond to the number of each vector in the projection basis.

### 3 FORCED RESPONSE

#### 3.1 Computation of the Generalized Aerodynamic Forces

The Generalized Aerodynamic Forces are obtained by CFD simulations, based on a 3D URANS approach. For each nodal diameter associated to the modes retained in the reduction basis, after projecting the appropriate mode shape onto the aerodynamic mesh, the unsteady pressure field is computed under the assumption of chorochronicity. Subsequently, the aeroelastic coefficients  $a_{\beta,k}^*$  are calculated by integrating the scalar product of the mode shape by the pressure field over the fluid-structure boundary:

$$a_{\beta,k}^* = \int_{\partial S} P^*(x,y,z) \Phi_{\beta,k}(x,y,z) \vec{n} \cdot d\vec{S} \quad (6)$$

In equation (6),  $P^*(x,y,z)$  and  $\Phi_{\beta,k}(x,y,z)$  correspond namely to the Fourier transform of the unsteady pressure field and to the projection over the aerodynamic mesh of the mode shape for the nodal diameter  $k$ .  $\partial S$  corresponds to the fluid-structure boundary, i.e. the blade surface.

The real part of  $a_{\beta,k}^*$  represents the flow contribution to the generalized stiffness of the structure for mode  $(\beta,k)$  whereas the imaginary part stands for the aerodynamic damping. Under the assumption of linearity, the dynamic equation of the coupled system (1) can be expressed in the modal domain:

$$([K] - \Omega^2[M] + i\omega[C] + [A] + i[B])\eta = \Phi^T f_{exc} \quad (7)$$

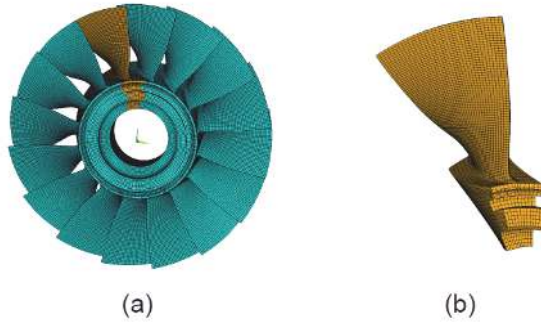
where  $[K]$  and  $[M]$  are the reduced stiffness and mass matrices and  $\eta$  represents the generalized coordinates. Since the vectors of the projection basis  $\Phi$  are not eigenvectors of the mistuned system, the matrices  $[K]$  and  $[M]$  are not diagonal. The following transformation is applied to the structural damping and aeroelastic coupling matrices:

$$\begin{aligned} [C] &= Z^{-T} \text{diag}(2\omega_i \zeta_i) Z^{-1} \\ [A] &= Z^{-T} \text{diag}(\text{Re}(a_{\beta,k}^*)) Z^{-1} \\ [B] &= Z^{-T} \text{diag}(\text{Im}(a_{\beta,k}^*)) Z^{-1} \end{aligned} \quad (8)$$

where  $Z = [z_1 \ \dots \ z_{\alpha}^*]$  is the basis of eigenvectors of the conservative reduced system:

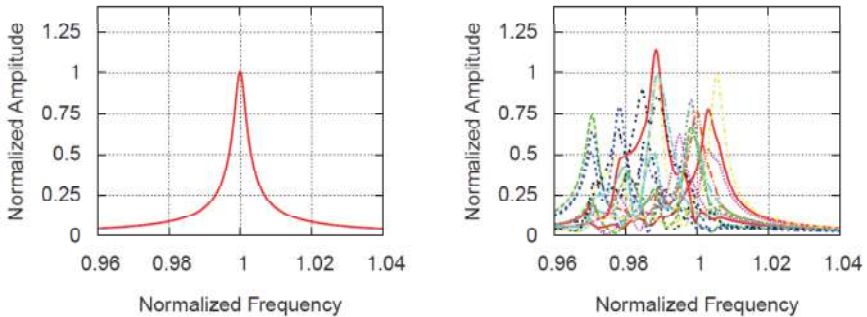
$$[K] z_i = \lambda_i [M] z_i \quad (9)$$

Figure 1 shows the finite element model of the industrial bladed disk on which this study focuses.



**Figure 1. Finite element model of the full bladed disk (a) and an arbitrary sector model (b) used for cyclic symmetry analyses**

The frequency response functions for an ideal, perfectly tuned structure and for the actual, geometrically mistuned bladed disk are shown in figure 2 and figure 3. The response amplitudes are normalized according to the peak value for the tuned structure.



**Figure 2. Frequency response function for tuned and mistuned bladed disks with aeromechanical coupling**

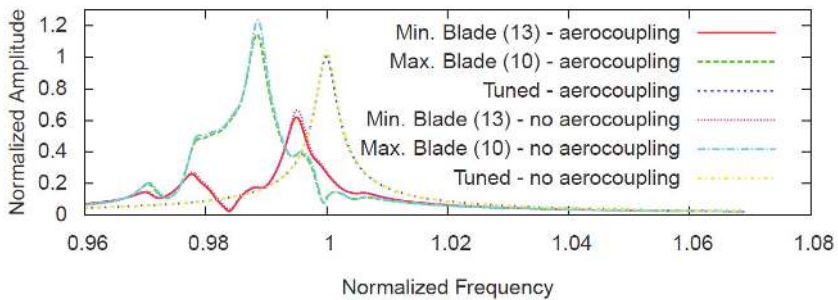


**Figure 3. Frequency response function for tuned and mistuned bladed disks with aeromechanical coupling**

From figure 2 it can be seen that the maximum amplification factor (defined as the ratio between the highest mistuned and tuned peak values) produced by geometric mistuning in presence of aeromechanical coupling has a value of 1.14. Figure 3 shows the impact of aeroelastic damping on the response of the tuned and

mistuned structures, for the blades that experience the highest and lowest response levels. It can be seen that the aeroelastic damping results in lower response amplitudes for all blades. At this stage of the current study, it should be noted that the aeroelastic forces are assumed to be symmetric, so that response localization only results from geometric mistuning.

### 3.2 Computation of the Aeroelastic Influence Coefficients

In this section, the formulation of the Aeroelastic Influence Coefficients is detailed, and emphasis is given on the perturbation of the Generalized Aerodynamic Forces through the Influence Coefficients Matrix, based on the approach introduced by Miyakozawa et al. [20, 13]. The aeroelastic coupling matrices obtained by CFD simulations (see section 3.1) are diagonal in the travelling wave modal space. One can write them in the modal physical space by means of a discrete inverse Fourier transform:

$$[A^*] = E^* [\hat{A}^*] E \quad (10)$$

In equation (10),  $[\hat{A}^*] = \text{diag}(a_{\beta,k}^*)$  is the complex Generalized Aerodynamic Forces matrix expressed in the travelling wave modal space, and  $E$  is the Fourier matrix:

$$E_{jk} = \frac{1}{\sqrt{N}} e^{\frac{2i\pi(j-1)(k-1)}{N}} \quad (11)$$

$[A^*]$  is the *Aeroelastic Influence Coefficients* matrix. Owing to the properties of Fourier matrices,  $[A^*]$  is circulant and generally dominated by tridiagonal terms [10, 13]. The Aeroelastic Influence Coefficients represent the level of blade-to-blade coupling due to fluid-structure interactions. Indeed, the diagonal influence coefficient  $a_{\beta,ii}^*$  corresponds to the aeroelastic force generated on blade  $i$  by its unit motion according to mode  $\beta$ , while the extradiagonal coefficient  $a_{\beta,ij}^*$  corresponds to the contribution of the modal motion of blade  $j$  to the aeroelastic force on blade  $i$ .

Figure 4 presents the normalized values of the Aeroelastic Influence Coefficients obtained from the Generalized Aerodynamic Forces calculated by CFD analyses on a basis sector of the actual bladed disk. It can be seen that matrix  $[A^*]$  is dominated by its diagonal coefficients. Therefore, only the latter will be kept as uncertain parameters in order to avoid excessive computational cost in the sensitivity study. Introducing random perturbations on at least one diagonal coefficient of matrix  $[A^*]$  lead to a non-circulant perturbed matrix  $[A_{per}^*]$ . A generalized perturbed aerodynamic forces matrix in travelling wave coordinates can be obtained by a direct discrete Fourier transform:

$$[\hat{A}_{per}^*] = E^* [A_{per}^*] E \quad (12)$$

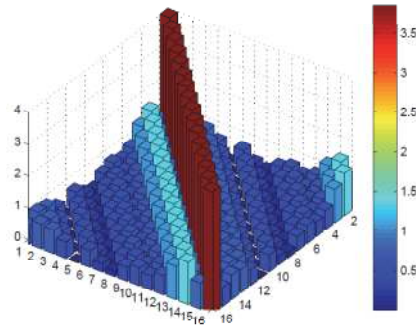


**Figure 4. Top view of aeroelastic influence coefficient matrix (modulus)  $|a_{\beta,ij}^*|$**



which is no longer diagonal. The matrix  $\begin{bmatrix} \hat{A}_{per}^* \end{bmatrix}$  represents the aerodynamic forces in travelling wave coordinates for non-symmetric flow conditions. Prior to solving the coupled problem, the aerodynamic perturbed stiffness and damping matrices in modal coordinates can be recovered from equation (8):

$$\begin{aligned} [A_{per}] &= Z^{-T} \left[ \text{Re}(\hat{A}_{per}^*) \right] Z^{-1} \\ [B_{per}] &= Z^{-T} \left[ \text{Im}(\hat{A}_{per}^*) \right] Z^{-1} \end{aligned} \quad (13)$$

#### 4 SENSITIVITY ANALYSIS

This section is devoted to the sensitivity study, which aims at ranking several uncertain parameters of the model (namely the Young's modulus, the structural modal damping ratio and the diagonal Aeroelastic Influence Coefficients) according to their influence on the maximum amplification factor. The present sensitivity study has been performed using the Morris OAT (Ones-At-a-Time) design. OAT designs consist in simulated experiments in which the impact of changing the values of each parameter is evaluated in turn [14]. Before initiating the sensitivity study, the space of uncertain parameters is sampled into  $r$  trajectories where each trajectory consists in a sequence of  $m$  designs. Afterwards, for each design  $x$ , the sensitivity indices associated to the uncertain variables are computed as follows [14]:

$$d_i(x) = \frac{[y(x_1, \dots, x_{i-1}, x_i + \Delta, x_{i+1}, \dots, x_k) - y(x)]}{\Delta} \quad (14)$$

where  $d_i(x)$  is the sensitivity index associated to variable  $i$  and  $y(x)$  is the maximum amplification factor calculated for design point  $x$ .  $\Delta$  is chosen so that  $(x_1, \dots, x_{i-1}, x_i + \Delta, x_{i+1}, \dots, x_k)$  remains in the allowed space of uncertain parameters. The global incidence of each parameter  $i$ ,  $1 \leq i \leq k$  over the response amplification can be characterized through the mean and standard deviations of the population of indexes calculated during the sensitivity analysis.

Table 1 presents the description, nominal values and variation ranges of the uncertain parameters retained for the sensitivity analysis.

**Table 1. Model input parameters for the global sensitivity analysis**

| Parameter    | Description                                 | Nominal value           | Range                           |     |
|--------------|---|-------------------------|---------------------------------|-----|
| $E$          | Young's modulus                             | $1.1 \times 10^5$ Mpa   | $[1.045:1.155] \times 10^5$ MPa | (1) |
| $\zeta$      | Modal damping ratio                         | $1.17 \times 10^{-3}$   | $[1.4:2.0] \times 10^{-3}$      | (2) |
| $ A_{ii}^* $ | Aeroelastic Influence Coefficient (modulus) | $5.4819 \times 10^{-5}$ | $[4.39:6.58] \times 10^{-5}$    | (3) |

(1) cf [21]

(2) cf [7]

(3) cf [13]

Figure 5 shows the ranking of the 18 variables according to the mean values of the sensitivity indices. It appears that the most influential parameters are the Aeroelastic Influence Coefficients associated to blades 9, 7 and 8. This result is consistent since these blades are close to the most amplified blade, i.e. blade 10.

According to the results of the Morris sensitivity analysis, the lack of knowledge on the modulus of elasticity has a very low influence over the maximum amplification factor. This can be explained by the fact that the geometric mistuning pattern is not considered as an uncertain parameter in the present study, and that the material properties are considered to be homogeneous. Indeed, in this study, the geometric mistuning for the considered bladed disk is taken into account as a deterministic parameter. Thus, the lack of knowledge about the structural stiffness only corresponds to a global variation of the Young's modulus for the whole bladed disk. Within the given range of variation, altering its value mainly results into a frequency shift and does not modify drastically the response amplitudes.

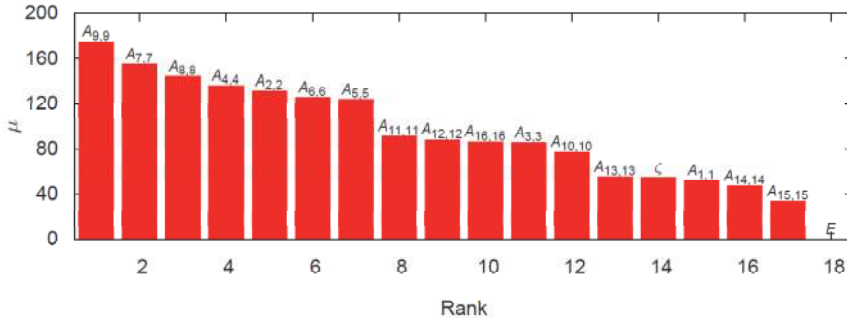


**Figure 5. Variable ranking**

The values of the means and standard deviations for the elementary effects of each variable are shown in figure 6. On the left plot, the plus representing the elementary effect of the modulus of elasticity is well separated from the group which is constituted of the effects of the damping and aeroelastic parameters, whose mean and standard deviation values are much higher. It can be seen on the right plot that the standard deviation value associated to the modal damping ratio is lower than those of the aeroelastic coefficients, which means that this parameter tends to influence in a linear and additive way the global output.

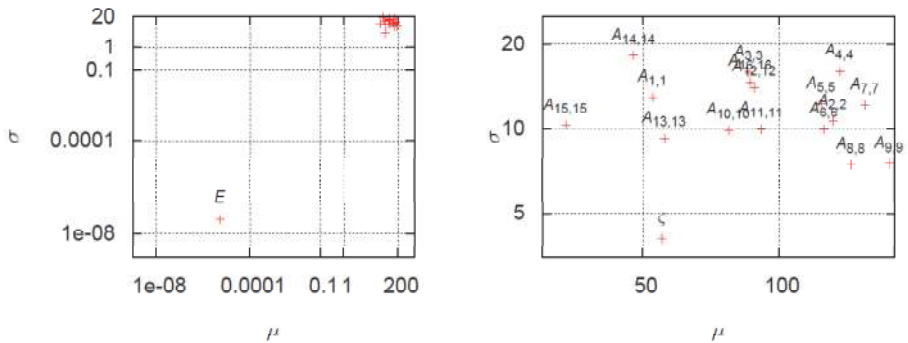


**Figure 6. Mean and standard deviation values of the elementary effects from the Morris sensitivity analysis**

Finally, figure 7 presents the scatterplot of the output for all the sampled values of the (9,9) aeroelastic coefficient, which is the most influential parameter. It can be seen that the amplification factor values reached during the sensitivity study span a range from 1.09 to 1.19. These results indicate that the contribution of the aeroelastic coefficients to the response of mistuned bladed disks is relevant, thus enforcing the need of increased computational efforts in order to characterize the variation of those coefficients due to geometric discrepancies.

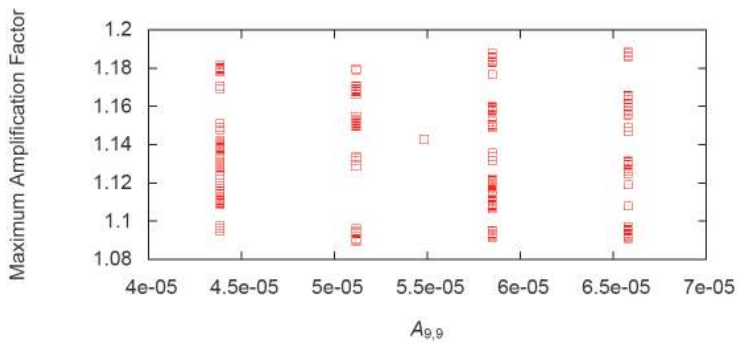


**Figure 7. Scatterplot of the maximum amplification factor values versus aeroelastic influence coefficient  $A_{9,9}$  sampled values**

## 5 CONCLUSION

In this paper, a methodology for studying the sensitivity of the forced response of a mistuned bladed disk to model uncertainties has been presented. Aerodynamic mistuning was taken into account by means of a perturbation approach applied to the Aeroelastic Influence Coefficients. It was found that, the Aeroelastic Influence Coefficients appear to be the most influent parameters according to their incidence over the maximum amplification factor for the given configuration where the structural mistuning pattern is considered as a deterministic parameter. As a consequence, the aim of our future research is to establish a more accurate characterization of the mistuned influence coefficients, and to assess the robustness of the forced response level calculations, considering the lack of knowledge on conservative and dissipative model parameters.

## 6 ACKNOWLEDGEMENTS

The Turbomeca Company is gratefully acknowledged for the permission to publish this work.

## 7 REFERENCE LIST

- [1] Rao, J. S., Turbomachine Blade Vibration, Wiley Western Limited, 1991.
- [2] Nikolic, M., New Insights into the Blade Mistuning Problem, PhD thesis, Imperial College of London, 2006.
- [3] Ewins, D. J. The effects of detuning upon the forced vibrations of bladed disks. *Journal of Sound and Vibration* 9 (1969).
- [4] Castanier, M. P. and Pierre, C. Modeling and Analysis of Mistuned Bladed Disk Vibration: Status and Emerging Directions *Journal of Propulsion and Power* 22 (2006).
- [5] Sinha, A., Hall, B., Cassenti, B., and Hilbert, G. Vibratory parameters of blades from coordinate measurement machine (CMM) data. *Journal of Turbomachinery* 130 (2008).
- [6] Schoenenborn, H., Grossmann, D., Satzger, W., and Zisik, H. Determination of Blade-Alone Frequencies of a Blisk for Mistuning Analysis Based on Optical Measurements. *ASME Conference Proceedings* 2009 (2009) 221.

- [7] Kielb, J. J. and Abhari, R. S. Experimental Study of Aerodynamic and Structural Damping in a Full-Scale Rotating Turbine. *ASME Journal of Engineering for Gas Turbines and Power* 125 (2003).
- [8] Srinivasan, A. V. Flutter and resonant vibration characteristics of engine blades. *Journal of Engineering for Gas Turbines and Power* 119 (1997).
- [9] Vahdati, M., Sayma, A. I., Imregun, M., and Simpson, G. Multibladerow Forced Response Modeling in Axial-Flow Core Compressors *Journal of Turbomachinery* 129 (2007).
- [10] Pierre, C. and Murthy, D. V. Aeroelastic Modal Characteristics of Mistuned Blade Assemblies : Mode Localization and Loss of Eigenstructure. *AIAA Journal* 30 (1992).
- [11] Crawley, E. F., *AGARD Manual on Aeroelasticity in Axial-Flow Turbomachines, Vol. 2, Structural Dynamics and Aeroelasticity*, pages 19–1 19–24, Advisory Group for Aerospace Research and Development, 1988.
- [12] Ekici, K., Kielb, R. E., and Hall, K. C. Aerodynamic Asymmetry Analysis of Unsteady Flows in Turbomachinery. *Journal of Turbomachinery* 132 (2010).
- [13] Miyakozawa, T., Kielb, R. E., and Hall, K. C. The Effects of Aerodynamic Asymmetric Perturbations on Forced Response of Bladed Disks. *Journal of Turbomachinery* 131 (2009).
- [14] Saltelli, A., Chan, K., and Scott, E. M. *Sensitivity Analysis*. John Wiley and Sons, 2000.
- [15] Sénéchal, P., *Dimensionnement des Turbomachines*, ENSAE, 1994.
- [16] Berthillier, M., Dhainaut, M., Burgaud, F., and Garnier, V. A Numerical Method for the Prediction of Bladed Disk Forced Response. *Journal of Engineering for Gas Turbines and Power* 119 (1997).
- [17] Mbaye, M., *Conception robuste en vibration et aéroélasticité des roues aubagées de turbomachines*, PhD thesis, Université Paris-Est, 2009.
- [18] Mbaye, M., Soize, C., and Ousty, J.-P. A reduced-order model of detuned cyclic dynamical systems with geometric modifications using a basis of cyclic modes. *Journal of Engineering for Gas Turbines and Power* 132 (2010).
- [19] Yang, M.-T. and Griffin, J. H. A Reduced-Order Model of Mistuning Using a Subset of Nominal System Modes. *Journal of Engineering for Gas Turbines and Power* 123, 2001.
- [20] Miyakozawa, T., *Flutter and Forced Response of Turbomachinery with Frequence Mistuning and Aerodynamic Asymmetry*, PhD thesis, Duke University, 2008.
- [21] Lemaitre, J. and Chaboche, J., *Mécanique des matériaux solides*, Dunod, 1988.